





ORIGINAL ARTICLE

MEK inhibition suppresses metastatic progression of *KRAS*-mutated gastric cancer

Juntaro Yamasaki¹ | Yuki Hirata² | Yuji Otsuki¹ | Kentaro Suina¹ | Yoshiyuki Saito²  | Kenta Masuda³  | Shogo Okazaki⁴ | Takatsugu Ishimoto⁵  | Hideyuki Saya¹ | Osamu Nagano¹ 

¹Division of Gene Regulation, Institute for Advanced Medical Research, School of Medicine, Keio University, Tokyo, Japan

²Department of Surgery, School of Medicine, Keio University, Tokyo, Japan

³Department of Obstetrics and Gynecology, School of Medicine, Keio University, Tokyo, Japan

⁴Division of Development and Aging, Research Institute for Biomedical Sciences, Tokyo University of Science, Noda, Japan

⁵Gastrointestinal Cancer Biology, International Research Center for Medical Sciences (IRCMS), Kumamoto University, Kumamoto, Japan

Correspondence

Osamu Nagano, Division of Gene Regulation, Institute for Advanced Medical Research, Keio University School of Medicine, 35 Shinano-machi, Shinjuku-ku, Tokyo 160-8582, Japan.
Email: osmna@sb3.so-net.ne.jp

Funding information

Japan Science and Technology Agency (JST) Moonshot R&D-MILLENNIA Program grant number JPMJMS2022-19 (to ON)

Abstract

Metastatic progression of tumors is driven by genetic alterations and tumor-stroma interaction. To elucidate the mechanism underlying the oncogene-induced gastric tumor progression, we have developed an organoid-based model of gastric cancer from Gastric Neoplasia (GAN) mice, which express Wnt1 and the enzymes COX2 and microsomal prostaglandin E synthase 1 in the stomach. Both p53 knockout (GAN-p53KO) organoids and *KRAS*^{G12V}-expressing GAN-p53KO (GAN-KP) organoids were generated by genetic manipulation of GAN mouse-derived tumor (GAN wild-type [WT]) organoids. In contrast with GAN-WT and GAN-p53KO organoids, which manifested Wnt addiction, GAN-KP organoids showed a Wnt-independent phenotype and the ability to proliferate without formation of a Wnt-regulated three-dimensional epithelial architecture. After transplantation in syngeneic mouse stomach, GAN-p53KO cells formed only small tumors, whereas GAN-KP cells gave rise to invasive tumors associated with the development of hypoxia as well as to liver metastasis. Spatial transcriptomics analysis suggested that hypoxia signaling contributes to the metastatic progression of GAN-KP tumors. In particular, such analysis identified a cluster of stromal cells located at the tumor invasive front that expressed genes related to hypoxia signaling, angiogenesis, and cell migration. These cells were also positive for phosphorylated extracellular signal-regulated kinase (ERK), suggesting that mitogen-activated protein kinase (MAPK) signaling promotes development of both tumor and microenvironment. The MEK (MAPK kinase) inhibitor trametinib suppressed the development of GAN-KP gastric tumors, formation of a hypoxic microenvironment, tumor angiogenesis, and liver metastasis. Our findings therefore establish a rationale for application of trametinib to suppress metastatic progression of *KRAS*-mutated gastric cancer.

KEYWORDS

epithelial-mesenchymal transition (EMT), gastric cancer, hypoxia, MEK, mouse model

Abbreviations: CD44, cluster of differentiation 44; HER2, human epidermal growth factor receptor 2; HIF1 α , hypoxia-inducible factor 1; NOD/SCID, Nonobese diabetic/severe combined immunodeficiency; VEGFA, vascular endothelial growth factor A.

This is an open access article under the terms of the Creative Commons Attribution-NonCommercial License, which permits use, distribution and reproduction in any medium, provided the original work is properly cited and is not used for commercial purposes.

© 2022 The Authors. *Cancer Science* published by John Wiley & Sons Australia, Ltd on behalf of Japanese Cancer Association.

1 | INTRODUCTION

Gastric cancer manifests highly heterogeneous molecular and histological features that reflect genetic and epigenetic alterations, and the existence of such tumor heterogeneity limits the effectiveness of cancer therapy.^{1,2} The *TP53* tumor suppressor gene is the most commonly mutated gene in human cancers.³ Mutations of this gene have been detected at the early stages of gastric adenocarcinoma and increase in frequency with tumor progression.⁴ Mutations of *KRAS* have also been identified in many human cancers and result in constitutive activation of downstream signaling pathways mediated by phosphatidylinositol 3-kinase (PI3K) and MAPK.^{5,6} Individuals with gastric cancer harboring the *KRAS*^{G12V} mutation have a shorter overall survival compared with those WT for *KRAS*.⁷

Wnt signaling plays an important role in homeostasis and regeneration of epithelial tissues.⁸ Activation of Wnt signaling allows epithelial stem cells to form three-dimensional (3D) epithelial organoids that recapitulate features of the original tissue architecture *in vitro*.^{9,10} Gastric organoids derived from gastric epithelial stem cells have therefore been established in Wnt-dependent 3D culture.^{11,12} Recently, the constitutive activation of Wnt signaling, which promotes self-renewal of gastric epithelial stem cells, cooperates with chronic inflammation to induce gastric tumorigenesis, has been confirmed in *K19-Wnt1/C2mE* mice (GAN mice), a transgenic model of gastric cancer induced by simultaneous activation of Wnt and prostaglandin E2 (PGE2) signaling pathways in gastric epithelium.¹³ However, the gastric tumors that develop in GAN mouse rarely show local invasion and metastasis,^{13,14} indicating that additional genetic or epigenetic events are required for further progression of the Wnt-induced gastric tumor.

CD44 is a major cell surface marker for cancer stem cells (CSCs) in gastric cancer.¹⁵ We have previously shown that a splice variant of CD44 (CD44v) interacts with and stabilizes the glutamate-cystine transporter xCT, resulting in increased intracellular levels of the major antioxidant glutathione and rendering cancer cells resistant to oxidative stress.¹⁶ In the GAN mouse, gastric tumors contain abundant CD44v-expressing stemlike tumor cells¹⁷ and genetic knock-out of CD44 markedly suppresses gastric tumor development,^{16,18} suggesting that the Wnt signaling activation in CD44v-expressing stemlike tumor cells might be essential for gastric tumorigenesis.

We have now investigated the impact of genetic alterations on tumor progression using the genetically engineered organoids derived from GAN mice and demonstrated that therapeutic targeting of MAPK signaling is effective for the suppression of metastatic progression of *KRAS*-mutated gastric cancer.

2 | MATERIALS AND METHODS

2.1 | Mice

K19-Wnt1/C2mE transgenic (GAN) mice were generated as described previously.¹⁸ C57BL/6J, BALB/c nu/nu, and NOD/SCID mice (CLEA, Japan) at 4–10 wk of age were used as recipients for

transplantation of organoid-derived tumor cells. All animal experiments were performed in accordance with protocols approved by the Ethics Committee of Keio University.

2.2 | GAN mouse-derived tumor organoids and cell culture

Isolation and organoid culture of tumor cells from GAN mice¹⁹ and establishment of GAN-p53KO cell and GAN-KP cells have been described previously.²⁰ For tracking these cells *in vivo*, we introduced GFP and luciferase reporter vectors into GAN-p53KO cells and the luciferase reporter vector into GAN-KP cells.

2.3 | Cell proliferation assay

Cells were seeded in 96-well plates (4000 cells per well) and subjected to 2D culture under 5% CO₂ at 37°C in DMEM supplemented with 10% FBS. Cell proliferation was analyzed with the use of a Cell Titer-Glo 2.0 luminescence-based cell viability assay kit (Promega).

2.4 | Plasmid construction

Complementary DNA for the G12V mutant of human *KRAS* was isolated from pGCDN-K-RasG12V-IRES-Kusabira Orange²¹ and was subcloned into the retroviral vector pMXs-IRES-GFP. The luciferase gene (*Luc2*) was subcloned into the retroviral vector pMXs-IRES-BSR (encoding a blasticidin resistance gene). Plat-E packaging cells (Cosmo Bio Co. LTD.) were transfected for 48 or 72 h with the resulting vectors with the use of the FuGene HD reagent (Promega), after which the retrovirus-containing culture supernatants were harvested for retroviral infection.

2.5 | In vivo drug treatment

GAN-KP cells (1×10^5 cells per site) were implanted into the gastric wall of athymic nude mice or C57BL6 mice, respectively. The mice were then assigned randomly to 2 groups for treatment with trametinib (1 mg/kg per day) by mouth for 21 d.

2.6 | Spatial transcriptomics

Spatial transcriptomics of the stomach transplanted with GAN-KP cells was performed using the 10x Genomics Visium platform (Visium, 10x Genomics). For gene ontology (GO) analysis, genes that were significantly upregulated in cluster 3 compared with the other clusters were identified and subjected to functional analysis with Database for Annotation, Visualization and Integrated Discovery (DAVID) Bioinformatics Resources 6.8 (<http://david.abcc.ncifcrf.gov>).

2.7 | Data availability

Microarray and spatial transcriptomics data are available in the Gene Expression Omnibus (GEO) database under the accession numbers GSE178087 and GSE186290, respectively. More detailed versions of methods and additional methodology are included in Supplementary Methods.

3 | RESULTS

3.1 | Oncogenic alteration of p53 and KRAS induces a Wnt-independent phenotype in gastric tumor cells

To study the impact of genetic alterations on gastric tumor progression, we used p53 knockout (GAN-p53KO) organoids and KRAS^{G12V}-expressing GAN-p53KO (GAN-KP) organoids that were generated by genetic manipulation of GAN mouse-derived tumor (GAN-WT) organoids (Figure S1A).^{18,19} The GAN-KP organoids underwent expansion at a markedly faster rate compared with GAN-WT or GAN-p53KO organoids (Figure S1B). H&E staining revealed that GAN-WT and GAN-p53KO organoids consisted mostly of a single-cell layer, whereas GAN-KP organoids developed as a multilayered mass consisting of cells with morphological abnormalities of the nucleus (Figure 1A). Furthermore, microarray analysis revealed that the expression of gastric differentiation marker genes^{22,23} was downregulated in GAN-KP organoids compared with GAN-WT and GAN-p53KO organoids (Figure 1B). Collectively, these results implicated that oncogenic alteration of KRAS and p53 results in the expansion of gastric tumor cells without cell differentiation.

The transfer of 3D-cultured gastric epithelial organoids to 2D cell culture in the presence of serum has been shown to trigger cell differentiation and limit cell proliferation.²⁴ We then subjected GAN-WT, GAN-p53KO, and GAN-KP cells to conventional 2D culture. Neither GAN-WT nor GAN-p53KO cells proliferated to a substantial extent under the differentiation-inducing 2D cell culture condition, whereas GAN-KP cells underwent robust proliferation (Figure 1C), suggesting that KRAS activation disrupts an epithelial polarity of gastric tumor cells and promotes an epithelial-mesenchymal transition (EMT)-like phenotypic change.

Adult gastrointestinal stem cell-derived organoids rely on the activation of Wnt/ β -catenin signaling for their propagation and maintenance of stemness.⁹ Given that *in vitro* propagation of GAN-KP cells did not require 3D organotypic culture (Figure 1C), we investigated the expression of genes related to the Wnt signaling pathway. Microarray analysis revealed that the expression of Wnt-related genes²⁵ was markedly attenuated in GAN-KP organoids compared with GAN-WT or GAN-p53KO organoids (Figure 1D). Furthermore, the proportion of cells showing localization of β -catenin in the nucleus was also greatly reduced for the GAN-KP organoids (Figure 1E). Together, these results suggested that Wnt/ β -catenin signaling is

less activated in GAN-KP cells compared with GAN-WT and GAN-p53KO cells.

To further confirm the Wnt-independent phenotype of GAN-KP cells, we examined the impact of XAV-939, an inhibitor of Wnt/ β -catenin signaling.²⁶ Whereas treatment with XAV-939 resulted in a significant reduction in the number of organoids formed by GAN-WT or GAN-p53KO cells, it had no such effect on organoid formation by GAN-KP cells (Figure 1F), suggesting that the maintenance and propagation of GAN-KP organoids are promoted by KRAS signaling independently of Wnt signaling activation.

CD44 expression is differentially regulated by Wnt/ β -catenin signaling²⁷ and oncogenic RAS.²⁸ To investigate the role of Wnt signaling in the maintenance of the undifferentiated state of GAN-KP organoids, we examined the effect of XAV-939 on the gene expression of a gastric CSC marker CD44. As the Wnt signaling inhibition by XAV-939 markedly reduced the cell viability of GAN-WT organoids (Figure 1F), we used GAN-p53KO and GAN-KP cells for such analysis. Whereas treatment with XAV-939 resulted in a significant decrease in the amount of CD44 mRNA in GAN-p53KO cells, it had no effect on that in GAN-KP cells (Figure 1G), indicating that CD44 expression in GAN-KP cells is regulated independently of Wnt signaling. We therefore examined the relevance of RAS-MAPK signaling to CD44 expression in GAN-KP cells. The MEK inhibitor U0126 markedly reduced the abundance of CD44 mRNA in GAN-KP cells (Figure 1G), suggesting that KRAS activation induced a phenotypic shift from Wnt addiction to Wnt independence and MAPK dependence in GAN mouse-derived tumor cells.

3.2 | GAN-KP cells give rise to invasive and metastatic gastric tumor

To investigate the behavior of GAN mouse-derived tumor cells *in vivo*, we introduced GFP and luciferase reporter vectors into GAN-p53KO cells and the luciferase reporter vector into GAN-KP cells (which already expressed GFP) for tracking tumor cells. At 21 d after injection of the manipulated cells into the serous side of gastric wall of syngeneic mice, bioluminescence imaging with luciferin revealed that GAN-KP cells gave rise to gastric tumors and liver metastases, whereas GAN-p53KO cells formed small tumors that could be detected only in the resected stomach (Figure 2A,B). Microscopic examination revealed liver metastasis in addition to the primary gastric tumors in recipients of GAN-KP cells, whereas mice injected with GAN-p53KO cells did not show metastasis in the liver. Furthermore, GAN-KP cells underwent lethal intraperitoneal metastasis after injecting the cells intraperitoneally, whereas GAN-p53KO cells did not (Figure S2A,B). Together, these results suggested that oncogenic KRAS conferred the ability to undergo invasive growth and metastasis in GAN mouse-derived tumor cells.

H&E staining and immunohistochemical analysis of GFP revealed that GAN-p53KO cells gave rise to small tumors that were composed of well differentiated tubular structures and presented only in the

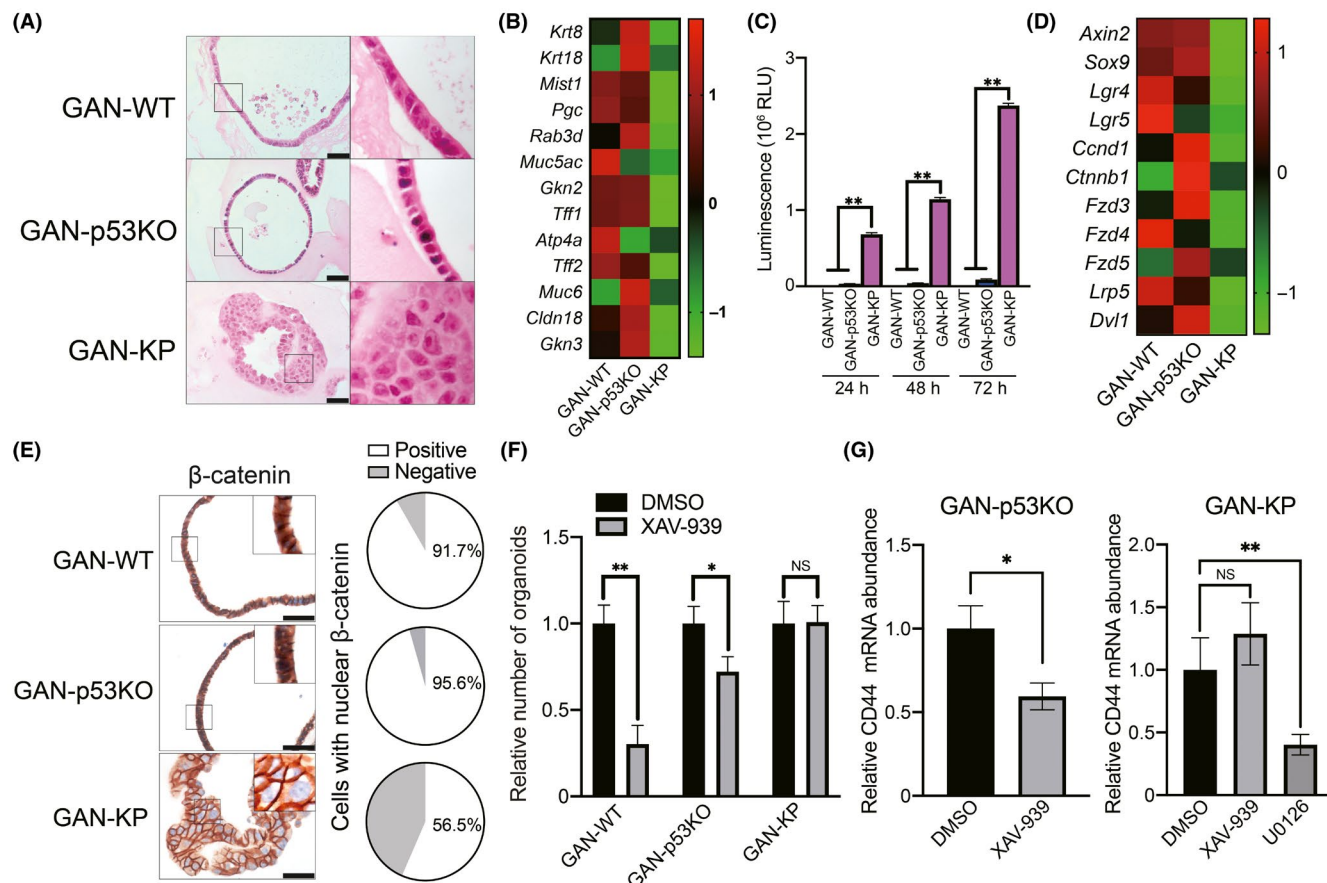


FIGURE 1 GAN-KP cells manifest a Wnt-independent phenotype. A, H&E staining of tumor organoids. Right panels show higher magnification of boxed regions. Scale bars, 50 μ m. B, Microarray analysis of gastric differentiation marker genes. Data are expressed as the Z-score and are presented as a heat map. C, Proliferation assay for GAN-WT, GAN-p53KO, and GAN-KP cells. Organoid-derived cells were subjected to 2D culture in DMEM supplemented with 10% FBS for 24, 48, or 72 h. Data are expressed as relative light units (RLU) and are means \pm SD for triplicate wells from a representative experiment. ** $P < .01$ (two-way ANOVA). D, Microarray analysis of the Wnt-related genes (Wnt target genes and Wnt signaling pathway genes). Data are expressed as the Z-score and are presented as a heat map. E, Immunohistochemical staining for β -catenin in the tumor organoids (left panels). The boxed regions are shown at higher magnification in the insets. Scale bars, 50 μ m. The proportion of cells showing nuclear localization of β -catenin is presented in the pie charts (right panels). F, Expansion of organoids in the presence of the Wnt signaling inhibitor XAV-939 (50 μ M) or dimethyl sulfoxide (DMSO) vehicle. Organoids with a diameter of ≥ 100 μ m were counted at 7 d after cell plating. Data are means \pm SD for triplicate wells of a representative experiment. * $P < .05$, ** $P < .01$; NS, not significant (two-way ANOVA). G, Quantitative RT-PCR analysis of CD44 mRNA abundance in GAN-p53KO (left panel) or GAN-KP (right panel) organoids cultured in the presence of XAV-939 (50 μ M), U0126 (10 μ M), or DMSO vehicle for 48 h. Data were normalized by the amount of β -actin mRNA and are means \pm SD from 3 independent experiments. * $P < .05$ (Student t test); ** $P < .01$, NS, not significant (one-way ANOVA)

injected site of gastric submucosa, whereas GAN-KP cells propagated throughout the stomach including the gastric mucosa after orthotopic transplantation (Figure 2C,D), indicating that GAN-KP cells were able to invade across the muscularis mucosa, a boundary between the mucosa and submucosa. Furthermore, unlike GAN-KP tumor tissue invading the gastric epithelium (GAN-KP-E), GAN-KP tumor tissue propagating in the submucosa (GAN-KP-S) contained large areas of necrosis (Figure 2D), suggesting that GAN-KP-S tumor tissue developed too rapidly for tumor angiogenesis to provide adequate support. Immunohistochemical analysis showed that both GFP-positive GAN-p53KO and GAN-KP tumor cells had high expression of CD44v in vivo (Figure 2C,D), suggesting that both these

tumor types contained CD44v-expressing gastric stemlike tumor cells.

Kaplan-Meier survival analysis revealed that orthotopic injection of GAN-KP cells markedly shortened the life span of recipient mice, whereas that of GAN-p53KO cells had no effect on mouse survival (Figure 2E). Furthermore, injection of GAN-KP cells into immunodeficient NOD/SCID mice shortened survival to an even greater extent compared with the immune competent C57BL/6J mice (Figure 2E). These results therefore suggested that the syngeneic mouse model based on the orthotopic transplantation of GAN-KP cells is likely to prove useful for studies on the progression of advanced gastric cancer in the presence of an intact immune system.

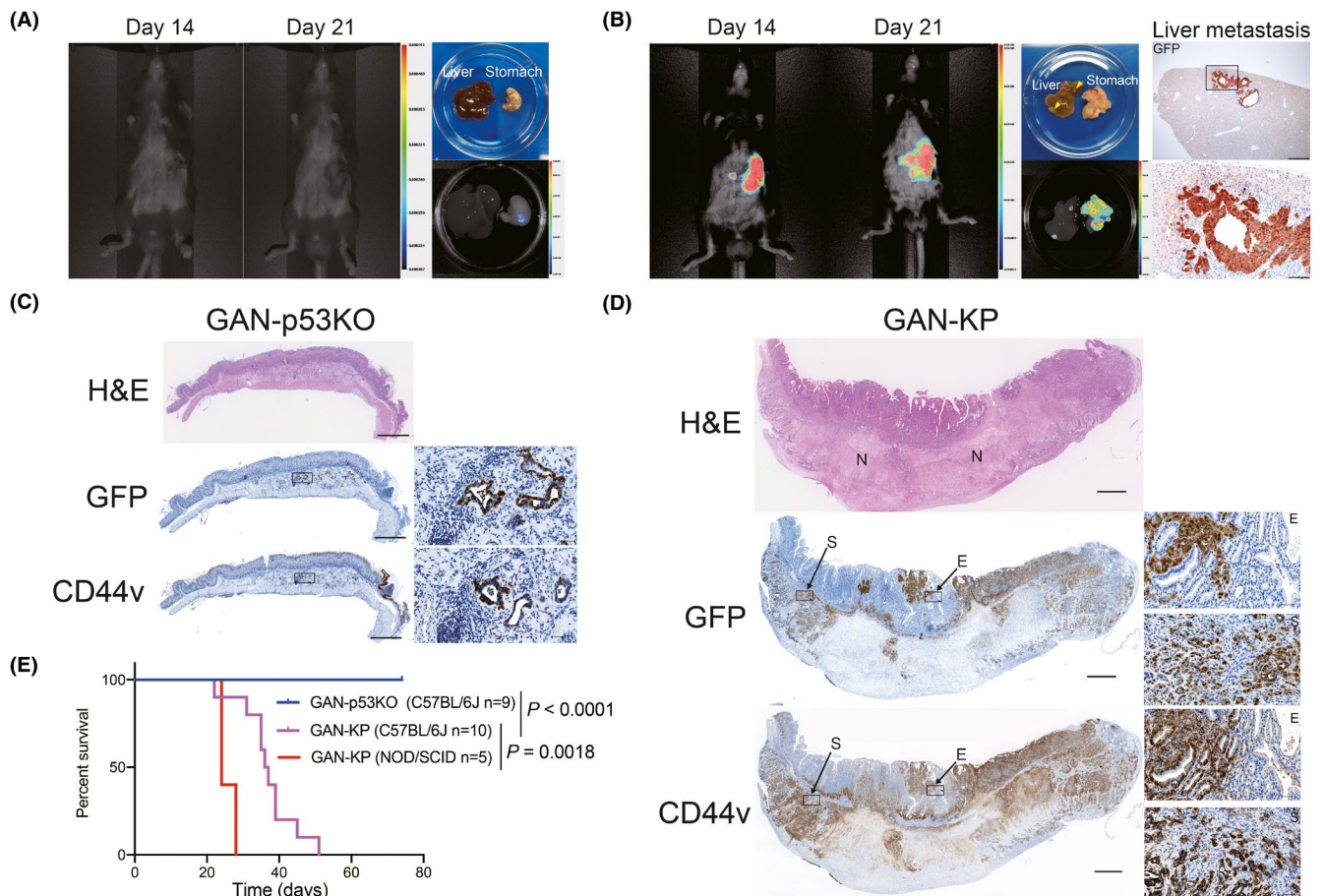


FIGURE 2 GAN-KP cells form invasive and metastatic gastric tumors. A, B, In vivo bioluminescence imaging of C57BL/6J mice at 14 and 21 d after orthotopic injection of GAN-p53KO (A) or GAN-KP (B) organoid-derived cells (1×10^5 per site) into the gastric wall (left). The macroscopic appearance and ex vivo bioluminescence imaging of the primary lesion and the liver at 21 d after cell injection are also shown (right in [A], center in [B]). The color scale and associated numbers indicate luminescence intensity level. Arrowheads indicate metastatic nodules in the liver (B). Immunohistochemical staining for GFP in liver metastatic tissue is also shown on the right in (B). The boxed region in the upper panel (scale bar, 500 μ m) is shown at higher magnification in the lower panel (scale bar, 100 μ m). C, D, Histology and immunohistochemical staining for GFP and CD44v in the stomach of syngeneic mice subjected to orthotopic transplantation of GAN-p53KO (C) or GAN-KP (D) cells (1×10^5 cells per site). Scale bars, 1 mm. The boxed regions are shown at higher magnification in the insets. Scale bars, 50 μ m. E, epithelium; N, necrotic region; S, submucosa. E, Kaplan-Meier curves of overall survival for syngeneic C57BL/6J mice subjected to orthotopic transplantation of GAN-p53KO ($n = 9$) or GAN-KP ($n = 10$) cells or for NOD/SCID mice subjected to orthotopic transplantation of GAN-KP cells ($n = 5$). The P -values were determined with the log-rank (Mantel-Cox) test

3.3 | Spatial transcriptomics showed hypoxia signaling is implicated in intratumoral heterogeneity

GAN-KP tumors frequently invaded the normal gastric epithelium after their injection into the stomach wall, resulting in the development of GAN-KP-E and GAN-KP-S tumor tissue in the mucosal lamina propria and submucosa, respectively (Figure 3A). Immunohistochemical analysis of GFP revealed that GAN-KP-E cells manifested collective invasion, a feature of epithelial-type cancer, whereas GAN-KP-S cells showed a single-cell invasion pattern, a feature of mesenchymal-type cancer²⁹ (Figure 3A), suggesting that the tumor microenvironment in the gastric mucosa and that in the submucosa have opposite effects on the EMT status of GAN-KP tumors.

To uncover the molecular mechanism underlying the intratumoral heterogeneity of GAN-KP tumors that manifests as GAN-KP-E

and GAN-KP-S tumor tissue, we performed spatial transcriptomics, which allows characterization of the spatial topography of gene expression.^{30,31} Such analysis allowed classification of the GAN-KP tumor cell population into 7 clusters, with high expression levels of *Epcam* (epithelial cell adhesion molecule) and *Cd44*, genes that are highly expressed in GAN-KP cells, identifying cluster 2 as a tumor cell population (Figure 3B, C). Furthermore, comparison between GAN-KP-E tumor tissue and adjacent GAN-KP-S tumor tissue within cluster 2 (Figure 3D) revealed that GAN-KP-S tumor cells expressed genes related to hypoxia, angiogenesis, and EMT at a higher level (Figure 3E). Given that the formation of GAN-KP-E tumor tissue is a consequence of the invasion of GAN-KP-S tumor cells into the gastric epithelium after injection of GAN-KP cells into gastric submucosa, these results suggested that the spatial topography of tumors influences intracellular signaling in the tumor cells.

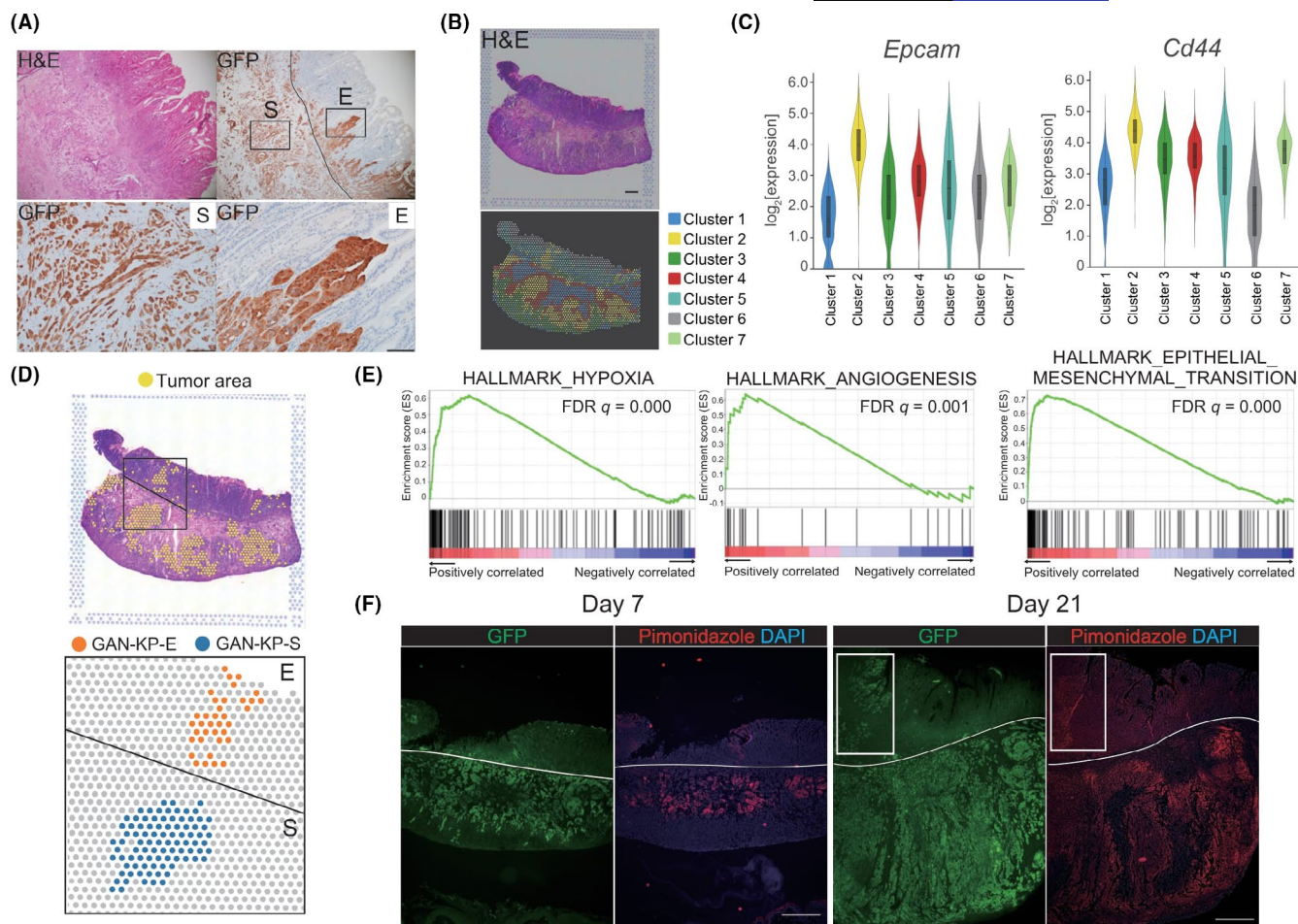


FIGURE 3 Spatial topography impacts intratumoral heterogeneity. A, H&E staining (upper left panel) and immunohistochemical staining of GFP (upper right panel) for the stomach of a C57BL/6J mouse subjected to orthotopic transplantation of GAN-KP cells (1×10^5 cells per site). Scale bars, 500 μ m. E, epithelium-invading GAN-KP-E cells; S, submucosa-invading GAN-KP-S cells. Lower panels show higher magnification of boxed regions in the upper right panel. Scale bars, 100 μ m. B, Visualization of the results for spatial gene expression analysis of a GAN-KP tumor. H&E staining (upper panel) and graph-based clustering (lower panel) are shown. Scale bar, 1 mm. C, Violin plots for *Epcam* and *Cd44* transcript abundance in the clusters. Most GAN-KP tumor cells are classified as cluster 2, which shows high expression of both *Epcam* and *Cd44* genes. D, Spatial transcriptomics of GAN-KP-E and GAN-KP-S tumor tissue. E, Gene set enrichment analysis (GSEA) of differentially expressed genes in GAN-KP-S vs GAN-KP-E was performed for hallmark collection gene sets (HALLMARK_HYPOXIA, HALLMARK_ANGIOGENESIS, and HALLMARK_EPITHELIAL_MESENCHYMAL_TRANSITION) downloaded from MSigDB (<https://www.gsea-msigdb.org/gsea/msigdb/genesets.jsp>). FDR, false discovery rate. F, Immunofluorescence staining of GFP (green) and pimonidazole (red) in the stomach of C57BL/6J mice at 7 and 21 d after orthotopic injection of GAN-KP cells (1×10^5 cells per site). Nuclei were stained with DAPI (blue). White rectangles indicate GAN-KP-E tumor tissue, with the white lines marking the boundary between the gastric mucosa and submucosa. Scale bars, 500 μ m

Hypoxia activates angiogenic pathways as well as the induction of EMT that leads to invasion and metastasis.^{32,33} To examine whether GAN-KP cells possess an ability to give rise to hypoxic microenvironment, we stained the GAN-KP tumor with a hypoxia probe pimonidazole. Immunofluorescence-based visualization of pimonidazole revealed hypoxia in the central region of GAN-KP-S tumor tissue at 7 d after cell transplantation and that this hypoxic area had extended from the central to the peripheral region of the tumor tissue at 21 d (Figure 3F). Collectively, these results suggested that GAN-KP tumors develop hypoxic microenvironment and thereby exhibit aggressive behaviors including angiogenesis and an EMT-like phenotype leading to metastasis.

3.4 | Trametinib suppresses hypoxia-promoted metastatic propagation of GAN-KP tumors

To investigate the functional relevance of MAPK signaling to metastatic tumor progression, we examined the phosphorylation status of ERK. The abundance of phosphorylated ERK (p-ERK) was increased in both stromal cells and tumor cells located at the invasive front of GAN-KP tumors (Figures 4A and S3A), suggesting that MAPK might play roles not only in tumor cells but also stromal cells at the invasion front.

To examine the tumor-stroma interaction at the invasive front of GAN-KP tumors, we analyzed cluster 3 identified in our spatial transcriptomics, which contains the p-ERK-positive stromal cells at the

invasive front of GAN-KP tumors (Figure 4B). GO analysis revealed that the stromal cells in cluster 3 manifested activation of genes related to cell adhesion, cell migration, angiogenesis, chemotaxis, and response to hypoxia relative to the other clusters (Figure 4B), suggesting that these p-ERK-positive stromal cells might contribute to the formation of the tumor-promoting stroma. The activation of individual genes related to angiogenesis, hypoxia signaling, and chemotaxis in stromal cells of cluster 3 was confirmed by visualization of their expression in spatial heat maps (Figure S3B). The stromal cells at the invasive front of

GAN-KP tumors also expressed HIF1 α and the angiogenesis markers VEGFA and CD31 (Figure 4C), suggesting that the activation of MAPK signaling in stromal cell might act synergistically with hypoxia signaling to support formation of a tumor-promoting microenvironment.

To investigate the potential of MAPK to serve as a therapeutic target for KRAS-mutated gastric cancer with large areas of hypoxic tissue, we examined the effects of the MEK inhibitor trametinib.^{34,35} Administration of trametinib significantly inhibited the formation of gastric tumors after syngeneic transplantation of GAN-KP cells

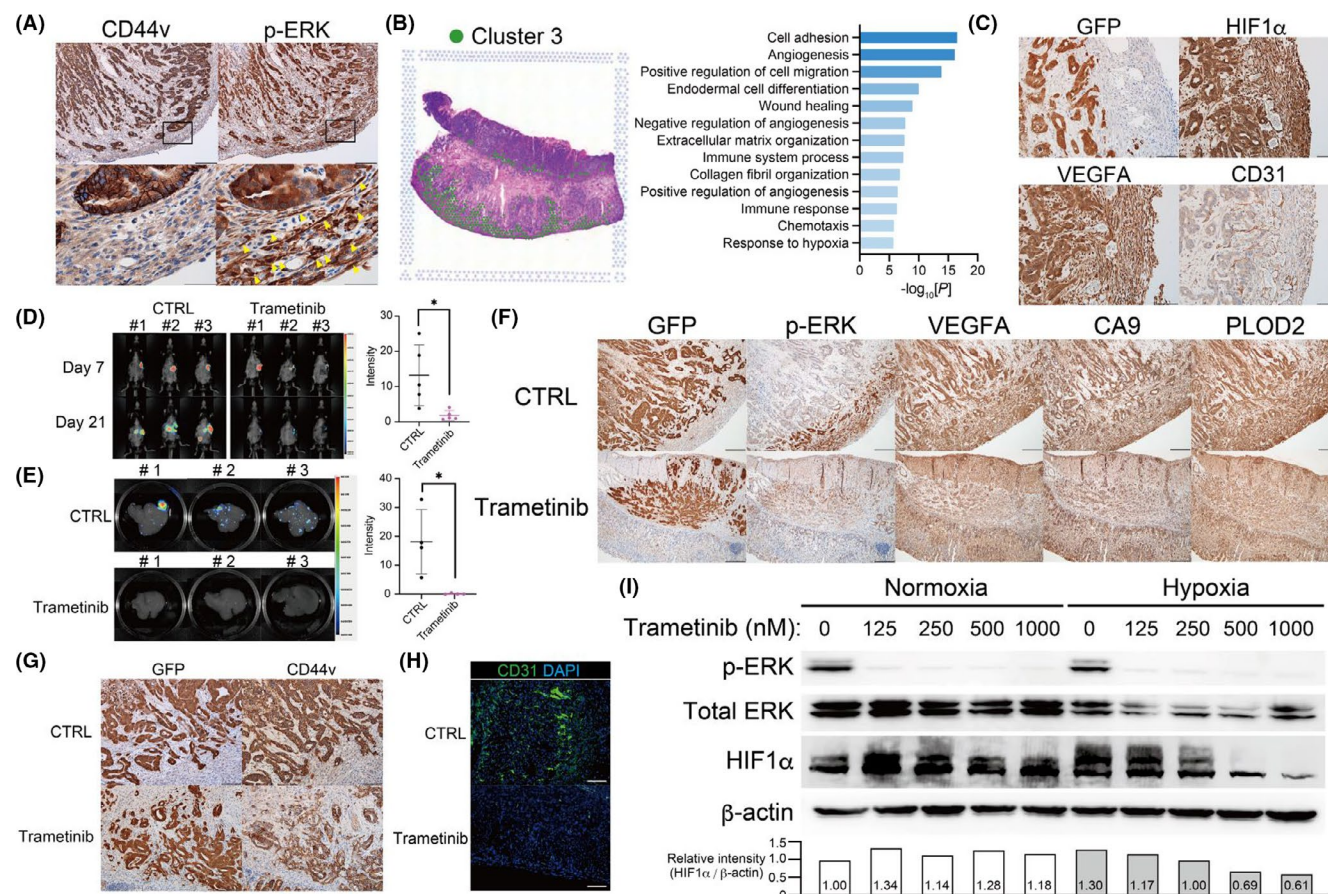


FIGURE 4 Trametinib suppresses hypoxia-promoted progression of GAN-KP tumor. A, Immunohistochemical staining of CD44v (upper left panel) and p-ERK (upper right panel) in the stomach of a C57BL/6J mouse subjected to orthotopic transplantation of GAN-KP cells (1×10^5 cells per site). Scale bars, 200 μ m. The boxed regions in the upper panels are shown at higher magnification in the lower panels. Arrowheads indicate p-ERK-positive stromal cells. Scale bars, 50 μ m. B, Spatial transcriptomics of cluster 3 as in Figure 3B (left) as well as GO functional analysis of genes that were highly expressed in cluster 3 relative to the other 6 clusters (right). C, Immunohistochemical staining of GFP, HIF1 α , VEGFA, and CD31 in GAN-KP tumors as in (A). Scale bars, 100 μ m. D, Effect of trametinib treatment on gastric tumors formed by GAN-KP cells (1×10^5 cells per site) after orthotopic transplantation into C57BL/6J mice. In vivo bioluminescence imaging of mice treated with trametinib or control (CTRL) was performed at 7 and 21 d after cell injection (left), and the luminescence intensity for the stomach on d 21 was quantified as mean \pm SD values for 5 mice (right). * $P < .05$ (Student *t* test). E, Effect of trametinib treatment on liver metastasis in BALB/c nu/nu mice after orthotopic transplantation of GAN-KP cells (1×10^5 cells per site). In vivo bioluminescence imaging was performed at 21 d after cell injection (left), and the luminescence intensity for the liver was quantified (right). Data were means \pm SD for 4 mice. * $P < .05$ (Student *t* test). F, Immunohistochemical staining of GFP, p-ERK, VEGFA, CA9, and PLOD2 in GAN-KP orthotopic tumors formed in C57BL/6J mice at 21 d after cell injection and treatment with trametinib or vehicle. Scale bars, 200 μ m. G, Immunohistochemical staining of GFP and CD44v in tumors of mice as in (F). Scale bars, 100 μ m. H, Immunofluorescence staining of CD31 (green) in tumors of mice as in (F). Nuclei were stained with DAPI (blue). Scale bars, 100 μ m. I, Immunoblot analysis of p-ERK, total ERK, HIF1 α , and β -actin (loading control) in GAN-KP cells cultured under the 2D condition for 18 h in the presence of the indicated concentrations of trametinib and then either maintained under the normoxic condition or exposed to hypoxia (1% O $_2$) for 6 h in the continued absence or presence of trametinib. The HIF1 α / β -actin band intensity ratio relative to the corresponding value for control (normoxia, w/o trametinib) are shown (lower panel)

(Figure 4D). Furthermore, trametinib completely suppressed liver metastasis of GAN-KP cells in immunodeficient nude mice, in which such metastasis occurs more frequently than in syngeneic mice (Figure 4E). These results therefore implicated MAPK signaling in the metastatic propagation of *KRAS*-mutated gastric tumor cells.

To examine whether MEK inhibition by trametinib affects formation of a hypoxic microenvironment in the stomach, we performed immunohistochemical analysis. The abundance of p-ERK as well as of the hypoxia-inducible proteins VEGFA, carbonic anhydrase 9 (CA9), and procollagen-lysine, 2-oxoglutarate 5-dioxygenase 2 (PLOD2) in stromal cells at the invasive front of GAN-KP gastric tumors was markedly reduced by trametinib administration (Figure 4F). Furthermore, the expression of CD44v in tumor cells (Figure 4G), as well as the number of CD31-positive vascular cells (Figure 4H) at the invasive front of GAN-KP tumors, were also attenuated by trametinib treatment, suggesting that MEK inhibition limited both the expansion of CD44v-expressing CSCs and the formation of a tumor-promoting microenvironment.

To determine whether MAPK signaling promoted HIF1 signaling, we exposed GAN-KP cells in 2D culture to normoxic or hypoxic (1%

O₂) conditions. The hypoxia-induced HIF1 α stabilization was inhibited by trametinib in a concentration-dependent manner (Figure 4I), suggesting that MEK plays a role in the cellular adaptation to hypoxia by promoting HIF1 α stabilization.

3.5 | MAPK and hypoxia signaling are implicated in the Wnt-independent progression of *KRAS*-mutated gastric cancer

To verify the impact of *KRAS* mutation on the phenotype of gastric cancer, we analyzed expression of a Wnt signaling pathway gene signature (KEGG_WNT_SIGNALING_PATHWAY) in the histologically defined human gastric adenocarcinoma specimens ($n = 177$) in The Cancer Genome Atlas (TCGA). The tumor samples were classified into high (Wnt-high) and low (Wnt-low) expression subgroups (Figure 5A), and most tumors harboring an activating mutation of *KRAS* (12 out of 13) were found to be present in the Wnt-low subgroup. Indeed, there was a statistically significant association

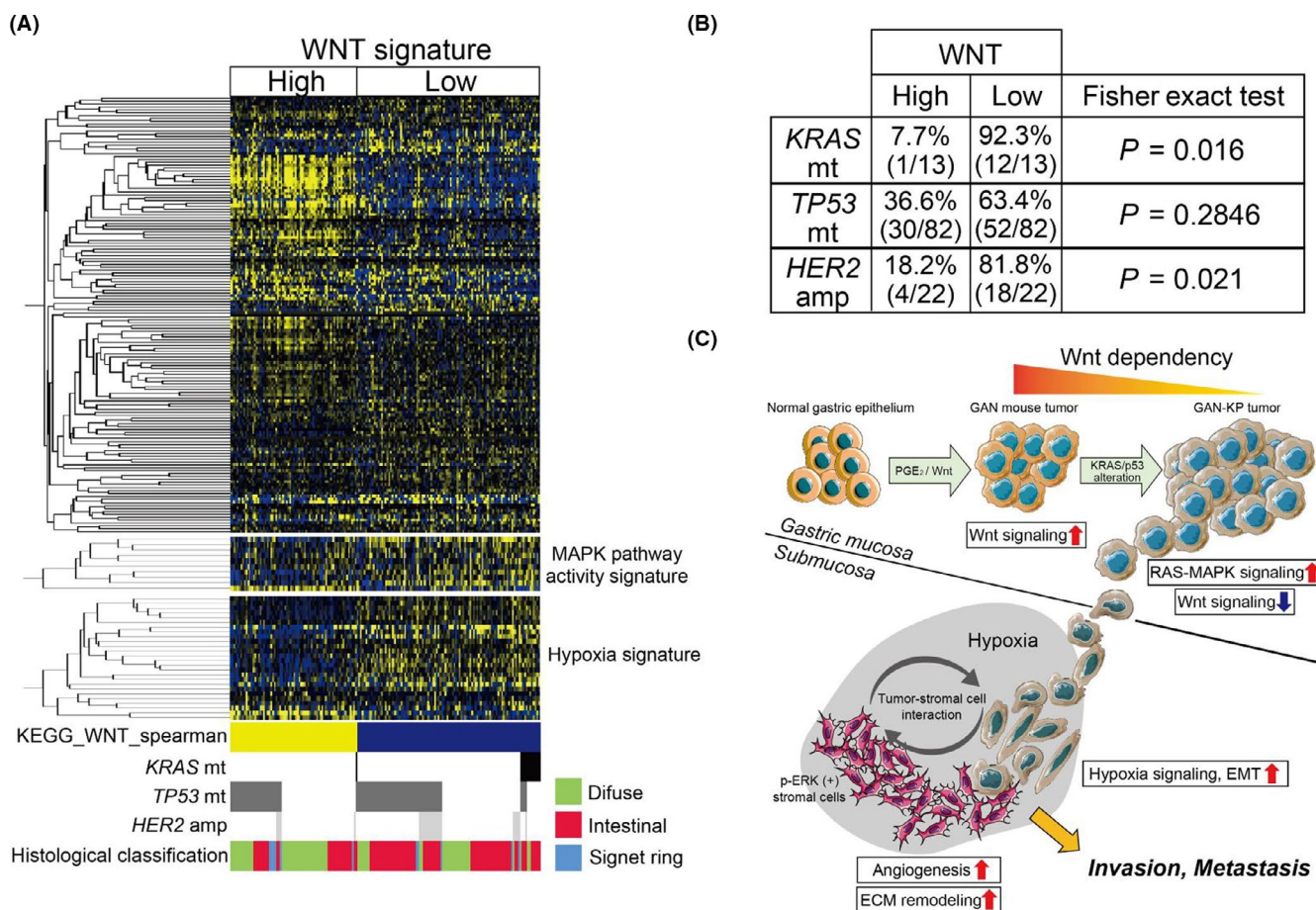


FIGURE 5 Gastric tumors with *KRAS* mutation or *HER2* amplification manifest reduced expression of Wnt signaling-related genes. A, Hierarchical clustering of differentially expressed genes related to Wnt signaling (KEGG_WNT_SIGNALING_PATHWAY) and a heat map for expression of 10 MAPK pathway activity-related genes and 26 hypoxia signature genes in the histologically defined tumors of TCGA data set ($n = 177$). Tumors positive for mutations (mt) of *KRAS* or *TP53* or for amplification (amp) of *HER2* as well as histological classification of the tumors are also indicated. B, The association of Wnt phenotype with *KRAS* mutation, *TP53* mutation, and *HER2* amplification. Statistical significance was determined with Fisher exact test. C, Schematic representation of the phenotypic shift from Wnt addiction to Wnt independence of *KRAS*-mutated tumor cells and hypoxia-promoted metastasis. ECM, extracellular matrix

between *KRAS* mutation and the Wnt-low phenotype, whereas no such association was apparent between *TP53* mutation and Wnt subgroups (Figure 5B), suggesting that activation of oncogenic *KRAS* signaling might promote gastric tumor progression in a Wnt-independent manner. Furthermore, amplification of *HER2* was also significantly associated with the Wnt-low phenotype (Figure 5A,B), suggesting that activation of MAPK signaling by *KRAS* mutation or *HER2* amplification promotes the development of gastric cancer in a manner independent of Wnt signaling activation.

Finally, we examined the relation of *KRAS* mutation to expression of gene signatures for MAPK pathway activation^{36,37} or hypoxia.³⁷ Gastric tumors with the Wnt-low phenotype, including most of the *KRAS*-mutated tumors, manifested higher expression of the MAPK pathway activation-related genes and hypoxia-related genes compared with Wnt-high tumors (Figure 5A), suggesting that Wnt-independent tumors positive for mutated *KRAS* tended to develop a hypoxic microenvironment and to progress in a manner dependent on crosstalk between MAPK and the hypoxia signaling pathways (Figure 5C).

4 | DISCUSSION

In the present study, we have now demonstrated that metastatic progression of GAN-KP tumor is dependent on both genetic alterations and the tumor microenvironment, and that hypoxia may play a key role in the Wnt-independent and MAPK-dependent progression of *KRAS*-driven gastric cancer.

Spatial transcriptomics is a method for spatial profiling of the transcriptome of cells within tissues.^{30,31} In the present study, we applied this method to examine differences in intracellular signaling that might contribute to the GAN-KP tumor progression. The submucosa-invading GAN-KP-S tumor cells expressed genes related to hypoxia signaling as well as to the hypoxia-associated processes of angiogenesis and EMT at a high level compared with the gastric epithelium-invading GAN-KP-E cells. Hypoxia develops in a highly proliferating mass of tumor cells that outgrows the tumor vasculature³⁸ and the resulting activation of hypoxia signaling contributes to the progression of cancers through activation of proliferative and angiogenic pathways, the induction of EMT, and the promotion of metastasis and immune evasion.^{32,33,39} It is possible that hypoxia-induced EMT confers a mesenchymal trait that allows GAN-KP tumor cells to propagate more quickly in submucosa. EMT has been identified as one of the features associated with poorly differentiated histology and poor outcome in human gastric cancer.^{40,41} Moreover, oncogenic transformation by *KRAS* mutation often occurs concomitantly with the induction of EMT in epithelial cells,^{42,43} suggesting that induction of the EMT program by *KRAS* signaling might be further enhanced by hypoxia. Furthermore, we showed that p-ERK, a marker of MAPK signaling activation, was expressed not only in GAN-KP tumor cells but also in stromal cells located at the invasive front. Such p-ERK-positive stromal cells preferentially expressed the genes associated with angiogenesis, extracellular

matrix organization, and hypoxia signaling. These results suggested that MAPK signaling plays a key role in the tumor-stroma interaction under hypoxia. In the present study, we demonstrated that the administration of trametinib, an inhibitor of MEK1 and MEK2 activity,^{34,35} inhibited the propagation and liver metastasis of GAN-KP gastric tumors. The GAN-KP tumor tissue of mouse treated with trametinib manifested a reduced abundance of p-ERK and CD44v, as well as of VEGFA and CA9, both of which are the products of HIF1 α target genes. Furthermore, trametinib markedly attenuated the stabilization of HIF1 α in GAN-KP cells exposed to hypoxia in vitro. Together, these results implicated MAPK signaling in the maintenance of undifferentiated gastric tumor cells and in the activation of HIF1 α -mediated hypoxia signaling.

Consistent with our results obtained with the GAN-KP model, the analysis of TCGA data set revealed that gastric tumors positive for mutated *KRAS* or *HER2* amplification, but not those with *TP53* mutations, manifested low expression of Wnt signature genes and high expression of a hypoxia-related gene signature, implicating that hypoxia signaling promotes Wnt-independent gastric cancer progression. Overall, our results suggested that hypoxia and MAPK signaling may play key roles in a Wnt-independent progression and trametinib might be effective for the suppression of hypoxia-promoted tumor-stroma interaction that leads to metastatic progression of *KRAS*-mutated gastric cancer.

ACKNOWLEDGMENTS

We thank I. Ishimatsu, M. Nishida, and H. Nakazawa for technical assistance as well as M. Kobori for help in preparation of the manuscript.

CONFLICTS OF INTEREST

The authors declare no conflicts of interest.

DATA AVAILABILITY STATEMENT

The data that support the findings of this study are available from the corresponding author upon reasonable request.

ORCID

Yoshiyuki Saito  <https://orcid.org/0000-0002-2462-6775>

Kenta Masuda  <https://orcid.org/0000-0003-4313-1636>

Takatsugu Ishimoto  <https://orcid.org/0000-0003-1852-1835>

Osamu Nagano  <https://orcid.org/0000-0002-7630-142X>

REFERENCES

1. Lauren P. The two histological main types of gastric carcinoma: diffuse and so-called intestinal-type carcinoma. an attempt at a histo-clinical classification. *Acta Pathol Microbiol Scand*. 1965;64:31-49.
2. Cancer genome atlas research N. Comprehensive molecular characterization of gastric adenocarcinoma. *Nature*. 2014;513:202-209.
3. Hollstein M, Sidransky D, Vogelstein B, Harris CC. p53 mutations in human cancers. *Science*. 1991;253:49-53.
4. Fenoglio-Preiser CM, Wang J, Stemmermann GN, Noffsinger A. TP53 and gastric carcinoma: a review. *Hum Mutat*. 2003;21:258-270.

5. Waters AM, Der CJ. KRAS. The critical driver and therapeutic target for pancreatic cancer. *Cold Spring Harb Perspect Med*. 2018;8:a031435.
6. Liu ZM, Liu LN, Li M, Zhang QP, Cheng SH, Lu S. Mutation detection of KRAS by high-resolution melting analysis in Chinese with gastric cancer. *Oncol Rep*. 2009;22:515-520.
7. Fu XH, Chen ZT, Wang WH, et al. KRAS G12V mutation is an adverse prognostic factor of Chinese gastric cancer patients. *J Cancer*. 2019;10:821-828.
8. Nusse R, Clevers H. Wnt/ β -catenin signaling, disease, and emerging therapeutic modalities. *Cell*. 2017;169:985-999.
9. Merenda A, Fenderico N, Maurice MM. Wnt signaling in 3D: recent advances in the applications of intestinal organoids. *Trends Cell Biol*. 2020;30:60-73.
10. Drost J, Clevers H. Organoids in cancer research. *Nat Rev Cancer*. 2018;18:407-418.
11. Barker N, Huch M, Kujala P, et al. Lgr5(+ve) stem cells drive self-renewal in the stomach and build long-lived gastric units in vitro. *Cell Stem Cell*. 2010;6:25-36.
12. Bartfeld S, Bayram T, van de Wetering M, et al. In vitro expansion of human gastric epithelial stem cells and their responses to bacterial infection. *Gastroenterology*. 2015;148:126-136.
13. Oshima H, Oguma K, Du YC, Oshima M. Prostaglandin E2, Wnt, and BMP in gastric tumor mouse models. *Cancer Sci*. 2009;100:1779-1785.
14. Poh AR, O'Donoghue RJ, Ernst M, Putoczki TL. Mouse models for gastric cancer: matching models to biological questions. *J Gastroenterol Hepatol*. 2016;31:1257-1272.
15. Lau WM, Teng E, Chong HS, et al. CD44v8-10 is a cancer-specific marker for gastric cancer stem cells. *Cancer Res*. 2014;74:2630-2641.
16. Ishimoto T, Nagano O, Yae T, et al. CD44 variant regulates redox status in cancer cells by stabilizing the xCT subunit of system xc(-) and thereby promotes tumor growth. *Cancer Cell*. 2011;19:387-400.
17. Ishimoto T, Oshima H, Oshima M, et al. CD44+ slow-cycling tumor cell expansion is triggered by cooperative actions of Wnt and prostaglandin E2 in gastric tumorigenesis. *Cancer Sci*. 2010;101:673-678.
18. Oshima H, Matsunaga A, Fujimura T, Tsukamoto T, Taketo MM, Oshima M. Carcinogenesis in mouse stomach by simultaneous activation of the Wnt signaling and prostaglandin E2 pathway. *Gastroenterology*. 2006;131:1086-1095.
19. Seishima R, Wada T, Tsuchihashi K, et al. Ink4a/Arf-dependent loss of parietal cells induced by oxidative stress promotes CD44-dependent gastric tumorigenesis. *Cancer Prev Res (Phila)*. 2015;8:492-501.
20. Okazaki S, Shintani S, Hirata Y, et al. Synthetic lethality of the ALDH3A1 inhibitor dyclonine and xCT inhibitors in glutathione deficiency-resistant cancer cells. *Oncotarget*. 2018;9:33832-33843.
21. Motohara T, Masuko S, Ishimoto T, et al. Transient depletion of p53 followed by transduction of c-Myc and K-Ras converts ovarian stem-like cells into tumor-initiating cells. *Carcinogenesis*. 2011;32:1597-1606.
22. Weis VG, Petersen CP, Mills JC, Tuma PL, Whitehead RH, Goldenring JR. Establishment of novel in vitro mouse chief cell and SPEM cultures identifies MAL2 as a marker of metaplasia in the stomach. *Am J Physiol Gastrointest Liver Physiol*. 2014;307:G777-792.
23. Noguchi TK, Ninomiya N, Sekine M, et al. Generation of stomach tissue from mouse embryonic stem cells. *Nat Cell Biol*. 2015;17:984-993.
24. Schlaermann P, Toelle B, Berger H, et al. A novel human gastric primary cell culture system for modelling *Helicobacter pylori* infection in vitro. *Gut*. 2016;65:202-213.
25. Fischer AS, Sigal M. The role of wnt and R-spondin in the stomach during health and disease. *Biomedicines*. 2019;7(2):44.
26. Huang SM, Mishina YM, Liu S, et al. Tankyrase inhibition stabilizes axin and antagonizes Wnt signalling. *Nature*. 2009;461:614-620.
27. Wielenga VJ, Smits R, Korinek V, et al. Expression of CD44 in Apc and Tcf mutant mice implies regulation by the WNT pathway. *Am J Pathol*. 1999;154:515-523.
28. Hofmann M, Rudy W, Günther U, et al. A link between ras and metastatic behavior of tumor cells: ras induces CD44 promoter activity and leads to low-level expression of metastasis-specific variants of CD44 in CREF cells. *Cancer Res*. 1993;53:1516-1521.
29. Friedl P, Locker J, Sahai E, Segall JE. Classifying collective cancer cell invasion. *Nat Cell Biol*. 2012;14:777-783.
30. Ståhl PL, Salmén F, Vickovic S, et al. Visualization and analysis of gene expression in tissue sections by spatial transcriptomics. *Science*. 2016;353:78-82.
31. Maniatis S, Åijö T, Vickovic S, et al. Spatiotemporal dynamics of molecular pathology in amyotrophic lateral sclerosis. *Science*. 2019;364:89-93.
32. Harris AL. Hypoxia—a key regulatory factor in tumour growth. *Nat Rev Cancer*. 2002;2:38-47.
33. Lu X, Kang Y. Hypoxia and hypoxia-inducible factors: master regulators of metastasis. *Clin Cancer Res*. 2010;16:5928-5935.
34. Gilmartin AG, Bleam MR, Groy A, et al. GSK1120212 (JTP-74057) is an inhibitor of MEK activity and activation with favorable pharmacokinetic properties for sustained in vivo pathway inhibition. *Clin Cancer Res*. 2011;17:989-1000.
35. Yamaguchi T, Kakefuda R, Tajima N, Sowa Y, Sakai T. Antitumor activities of JTP-74057 (GSK1120212), a novel MEK1/2 inhibitor, on colorectal cancer cell lines in vitro and in vivo. *Int J Oncol*. 2011;39:23-31.
36. Wagle MC, Kirouac D, Klijn C, et al. A transcriptional MAPK pathway activity score (MPAS) is a clinically relevant biomarker in multiple cancer types. *NPJ Precis Oncol*. 2018;2:7.
37. Eustace A, Mani N, Span PN, et al. A 26-gene hypoxia signature predicts benefit from hypoxia-modifying therapy in laryngeal cancer but not bladder cancer. *Clin Cancer Res*. 2013;19:4879-4888.
38. Brahimi-Horn MC, Chiche J, Pouyssegur J. Hypoxia and cancer. *J Mol Med (Berl)*. 2007;85:1301-1307.
39. Kerk SA, Papagiannakopoulos T, Shah YM, Lyssiotis CA. Metabolic networks in mutant KRAS-driven tumours: tissue specificities and the microenvironment. *Nat Rev Cancer*. 2021;21:510-525.
40. Kim MA, Lee HS, Lee HE, Kim JH, Yang HK, Kim WH. Prognostic importance of epithelial-mesenchymal transition-related protein expression in gastric carcinoma. *Histopathology*. 2009;54:442-451.
41. Oh SC, Sohn BH, Cheong JH, et al. Clinical and genomic landscape of gastric cancer with a mesenchymal phenotype. *Nat Commun*. 2018;9:1777.
42. Singh A, Greninger P, Rhodes D, et al. A gene expression signature associated with "K-Ras addiction" reveals regulators of EMT and tumor cell survival. *Cancer Cell*. 2009;15:489-500.
43. Shao DD, Xue W, Krall EB, et al. KRAS and YAP1 converge to regulate EMT and tumor survival. *Cell*. 2014;158:171-184.

SUPPORTING INFORMATION

Additional supporting information may be found in the online version of the article at the publisher's website.

How to cite this article: Yamasaki J, Hirata Y, Otsuki Y, et al. MEK inhibition suppresses metastatic progression of KRAS-mutated gastric cancer. *Cancer Sci*. 2022;113:916-925. doi:[10.1111/cas.15244](https://doi.org/10.1111/cas.15244)